

NRC Publications Archive Archives des publications du CNRC

CAD/CAM framework for generation of surface microstructures through elliptical vibration assisted single point cutting

Farrus, Nikolai; Tutunea-Fatan, Remus; Bordatchev, Evgueni

This publication could be one of several versions: author's original, accepted manuscript or the publisher's version. / La version de cette publication peut être l'une des suivantes : la version prépublication de l'auteur, la version acceptée du manuscrit ou la version de l'éditeur.

For the publisher's version, please access the DOI link below. / Pour consulter la version de l'éditeur, utilisez le lien DOI ci-dessous.

Publisher's version / Version de l'éditeur:

<https://doi.org/10.14733/cadaps.2021.669-681>

Computer-Aided Design and Applications, 18, 4, pp. 669-681, 2020-11-10

NRC Publications Archive Record / Notice des Archives des publications du CNRC :

<https://nrc-publications.canada.ca/eng/view/object/?id=4f5e119c-14f2-4a6f-a356-668410ef8694>

<https://publications-cnrc.canada.ca/fra/voir/objet/?id=4f5e119c-14f2-4a6f-a356-668410ef8694>

Access and use of this website and the material on it are subject to the Terms and Conditions set forth at

<https://nrc-publications.canada.ca/eng/copyright>

READ THESE TERMS AND CONDITIONS CAREFULLY BEFORE USING THIS WEBSITE.

L'accès à ce site Web et l'utilisation de son contenu sont assujettis aux conditions présentées dans le site

<https://publications-cnrc.canada.ca/fra/droits>

LISEZ CES CONDITIONS ATTENTIVEMENT AVANT D'UTILISER CE SITE WEB.




Questions? Contact the NRC Publications Archive team at

PublicationsArchive-ArchivesPublications@nrc-cnrc.gc.ca. If you wish to email the authors directly, please see the first page of the publication for their contact information.

Vous avez des questions? Nous pouvons vous aider. Pour communiquer directement avec un auteur, consultez la première page de la revue dans laquelle son article a été publié afin de trouver ses coordonnées. Si vous n'arrivez pas à les repérer, communiquez avec nous à PublicationsArchive-ArchivesPublications@nrc-cnrc.gc.ca.



CAD/CAM Framework for Generation of Surface Microstructures through Elliptical Vibration Assisted Single Point Cutting

Nikolai Farrus^{1*} , O. Remus Tutunea-Fatan^{2*}  and Evgueni Bordatchev^{3*} 

¹Western University, nfarrus@uwo.ca

²Western University, rtutunea@eng.uwo.ca

³National Research Council of Canada, evgueni.bordatchev@nrc-cnrc.gc.ca

Corresponding authors: O. Remus Tutunea-Fatan, rtutunea@eng.uwo.ca
Evgueni Bordatchev, evgueni.Bordatchev@nrc-cnrc.gc.ca

Abstract. Elliptical vibration assisted single point cutting (EVASPC) combines the kinematics of the 'slow' motion characteristic to conventional multi-axis CNC machines with that of the 'ultrafast' motion associated with ultrasonic elliptical vibrations. The summation of the slow and ultrafast motions results in a discontinuous contact between the cutting tool and the workpiece. This type of interrupted cut proved to be particularly advantageous in micro/nano fabrication of ferrous and other hard-to-cut materials. The primary objective of this study was to create a CAD/CAM framework capable to capture the aforementioned kinematic motions as well as predict the resulting surface. The developed framework was tested for a number of cutting strategies by means of analytical and geometric models that were subsequently validated by means of physical specimens replicating the targeted surface topography. The practical implementations of EVASPC demonstrated in this study include an optical surface quality surface ($S_a < 14$ nm), diffraction gratings, and saw-tooth microstructures, all with potential in various industrial applications.

Keywords: micro/nano machining, elliptical vibration cutting, single point cutting, process parameters, surface topography

DOI: <https://doi.org/10.14733/cadaps.2021.669-681>

1 INTRODUCTION

Recent years have shown an increased demand for single point cutting methods that are capable of generating surfaces characterized by a broad range of functionalities, such as improved optical surface quality, paintless coloring, wettability, and micro surface texturing. While such functionalities can be obtained, certain conventional single point cutting (SPC) technological limitations continue to hinder further developments. Among them, the dimensional barrier (i.e., the capability to produce

* All authors have contributed equally to the manuscript.

precise micro/nano-structures) as well as the ability to machine ferrous or other hard-to-cut materials by means of diamond tools continue to remain important challenges.

To address them, one possibility proposed is represented by the use of elliptical vibration cutting (EVC) as a technology capable of augmenting the previously proposed ultraprecise single point cutting method (USPC) [9]. Along these lines, elliptical vibration assisted single point cutting (EVASPC) constitutes a combination of SPC and EVC motions. In this context, the multi-axis stage of the five-axis machine is used to generate SPC kinematics in a manner similar to conventional cutting (CC) methods. By contrast, EVC motions are controlled externally (by the EVC unit), generating elliptical motion with micron-scale amplitudes at kHz-scale frequencies. The main role of the fast EVC motion is to introduce discontinuities in the tool/workpiece contact and thereby convert the continuous cutting into a discontinuous one. The intermittent tool/workpiece contact ultimately leads to smaller cutting forces, reduced tool wear and temperature gradients, all factors that essentially extend the applicability of EVC to ferrous and/or hard-to-cut materials.

Elliptical vibration cutting has been introduced in many industrial applications. Some of the early uses of EVC were focused on obtaining optical surface quality at a time when this was believed to be a technological impossibility [10]. Subsequent attempts have extended the range of application of EVC to 'paintless coloring' of metallic surfaces, one of the first practical demonstrations of micro diffraction gratings [12]. Other EVC implementations illustrated its capability with respect to sinusoidal, ramp, zig-zag and trapezoidal surface texturing, particularly with respect to microstructures that can be used to enhance surface functionality/wettability. The generation of such microgeometries relied on micro/nano elliptical amplitude modulation in order to control the depth-of-cut across the cutting length [13]. Similarly, phased-shift controlled elliptical vibration cutting proved to be able to augment the wettability and hydrophobic/hydrophilic properties of the surface, especially since the control of the spatial orientation of the ellipse can also be achieved [6]. Nonetheless, although elliptical vibration cutting has made significant advancements over the past years, it appears that some of the traditional SPC applications such as retroreflective lighting [7], bio-mimicry [1], and enhanced hydrodynamics and aerodynamics [8] could still benefit from EVC's improved surface quality and functionalization characteristics.

It is important to emphasize here that all CAD/CAM models that were proposed in the past for EVASPC-focused studies could be regarded as 'local' or 'punctiform' solutions to the problem at hand. For instance, the study presented in [16] demonstrated the impact of tool edge radius on surface profile by developing a 2D model to simulate the corresponding surface roughness. Similarly, the work detailed in [15] proved the effectiveness of cutting compensation in the general context of EVASPC, whereas others researchers have relied on 2D and 3D simulations/computations of surface topography in order to compare them with their physical correspondents [5]. Nonetheless, the analytical/theoretical models proposed so far lack the ability to handle a wide range of EVASPC parameters in order predict their effect on the resulting surface topography.

Building on this, the main objective of the present study was to propose a common CAD/CAM framework capable to integrate different implementations of EVASPC. The novelty of the work resides precisely in the development of a generalized CAD/CAM approach to be used towards the generation of surface microstructures by means of a specific EVASPC implementation tailored to a specific application and/or functional requirement: surface quality, regular/variable linear/spatial nano-/micro-structuring, etc. The framework to be detailed further will be based on analytical representations of the tool motion and will be used to generate geometric models of the resulting surface topography as well as to demonstrate EVASPC applicability with respect to physical specimens. The kinematic formulations to be presented herein will encompass the general equations of motion for EVC to be essentially determined by the superposition between the slow motion of the CNC stage ('stage motion cutting' = SMC) and the ultrafast EV motion. Based on this, four different EVASPC implementations will be introduced, each driven by a different set of motion control parameters. Finally, the outcome of the proposed CAD/CAM framework will be exemplified both by means of geometric models and physical surface topographies.

2 ANALYTICAL MODELING OF EVASPC KINEMATICS

The kinematic description of EVASPC constitutes the mathematical scaffold for various implementations of this technology. As indicated above, two overlapped primary motions form the core of this cutting technique: the slow (usually translational) motions of the stage and the ultrafast EV motions. The slow motions are provided by the intrinsic kinematics of the machine tool and they are characteristic to conventional 'no-EVC' three-axis CNC machining. On the other hand, ultrafast EV motions are generated by means of an external device (Figure 1).

The separation of slow and ultrafast motion components enables the further analysis of its kinematic components $x(t), y(t), z(t)$. In this regard, it can be noticed that SMC are controlled by two main parameters, namely stage velocity/feed (V_{SMC}) and depth of cut (DoC).

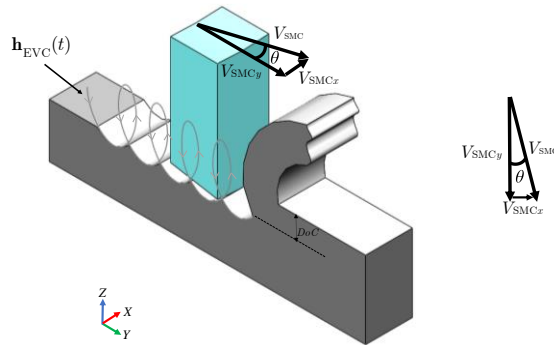


Figure 1: EVASPC kinematics obtained through the superposition of SMC and EVC.

The SMC components are detailed in Equation (2.1)

$$\begin{aligned}x_{SMC}(t) &= V_{SMC} \cdot \sin(\theta)t \\y_{SMC}(t) &= V_{SMC} \cdot \cos(\theta)t \\z_{SMC}(t) &= DoC\end{aligned}\quad (2.1)$$

where t represents time. An additional – yet rarely used – parameter termed as feed angle (θ) is defined between the direction of V_{SMC} and that of the plane containing the EV motion. The feed rate V_{SMC} can either be constant or variable with respect of time and same applies to DoC . However - as Eq. 2.1 implies - the current study will assume V_{SMC} and DoC as constant as well as $\theta = 0$. Any deviations from these assumptions could constitute the object of future extensions of this work.

By contrast, the ultrafast EV component $\mathbf{h}_{EVC}(t)$ is introduced by means of an external motion generator as follows:

$$\begin{aligned}x_{EVC}(t) &= 0 \\y_{EVC}(t) &= A_y \cos(2\pi\omega t + \phi_y) \\z_{EVC}(t) &= A_z \sin(2\pi\omega t + \phi_z)\end{aligned}\quad (2.2)$$

According to Equation (2.2), EVC is a planar motion that remains contained in the YZ plane. The ultrafast EV motion is defined by three primary parameters described further. The bending and longitudinal amplitudes (A_y and A_z respectively) are the primary variables associated with the elliptical motion. More specifically, the bending amplitude (A_y) represents the amplitude in the

direction parallel to feed, whereas the longitudinal amplitude (A_z) is perpendicular to feed. Both amplitudes can be constant in time (thus yielding uniform ellipses), or can be variable (thus enabling the amplitude modulation of the EV motion). In addition to the two amplitudes, the vibrational frequency of the EV motion (ω) is a fixed parameter that is based on capabilities of the EV generator. Finally, the third defining parameter of the EV motion is the phase angle (ϕ_y, ϕ_z) that defines the relative spatial orientation between A_y and A_z . The overlap between SMC and EVC can be graphically represented as depicted in Figure 2.

The combination between SMC and EVC as well as the relative positioning between the planes in which they occur cause the tip of the cutting tool to follow a trochoidal path (Figure 1). Equation (2.3) integrates these two motions and covers all possible variants offered in this cutting technology.

$$\mathbf{h}(t) = \begin{cases} x(t) = \mathbf{V}\sin(\theta)t \\ y(t) = \mathbf{V}\cos(\theta)t + A_y\cos(2\pi\omega t + \phi_y) \\ z(t) = DoC + A_z\sin(2\pi\omega t + \phi_z) \end{cases} \quad (2.3)$$

Table 1 identifies four primary and common implementations of EVASPC, all derived from Equation (2.3). According to this, the first implementation can be obtained by simply keeping all SMC and EVC parameters constant. This will lead to spatially uniform structures and consistent surface topography, as shown in the past [10].

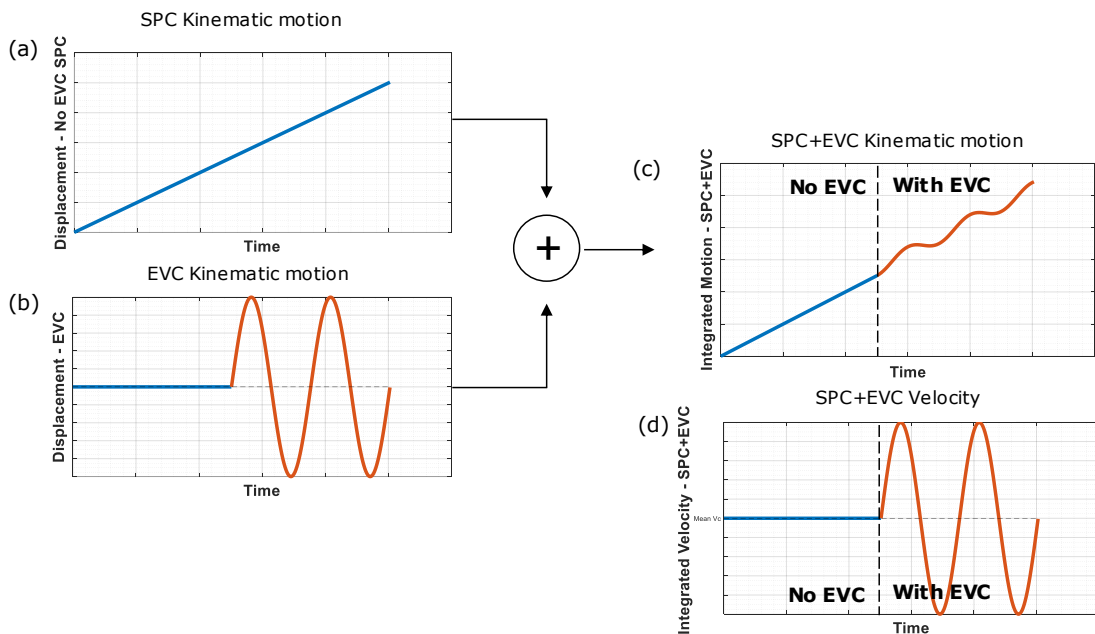


Figure 2: EVASPC motion characteristics: (a) no-EVC SPC kinematics, (b) EVC kinematics, (c) integrated EVASPC kinematics, and (d) integrated EVASPC velocity.

The second implementation - demonstrated by Yang et al. [12] - assumes a linear variation of the feed rate (V_c) and in turn, this allows for the introduction of areally-distributed frequency modulation. The third implementation relies on the control of the vibrational amplitudes (A_y, A_z),

consequently modulating DoC across the cutting area. This approach was used in the past to create sinusoidal, ramp and zigzag surface geometries [14].

		EVASPC Parameters					
		V_{SMC}	A_y, A_z	(ϕ_y, ϕ_z)	DoC	ω	θ
Implementation	1	const	const	const	const	const	0
	2	var	const	const	const	const	0
	3	const	var	const	const	const	0
	4	const	const	var	const	const	0

Table 1: Possible EVASPC implementations.

The fourth strategy - arguably the most difficult and advanced strategy encompassed by Equation (2.3) - involves modulation of ellipse orientation. This can be achieved by modifying the phase shift between bending and longitudinal amplitudes of the ellipse. This will change its orientation from forward-tilted, to vertical or even back-tilted. This implementation facilitates generation of periodical structures with a directional controlled of their inclination [6].

Equation (2.3) enables the synthesis of the proposed CAD/CAM framework (Figure 3) to be further exploited in the upcoming sections.

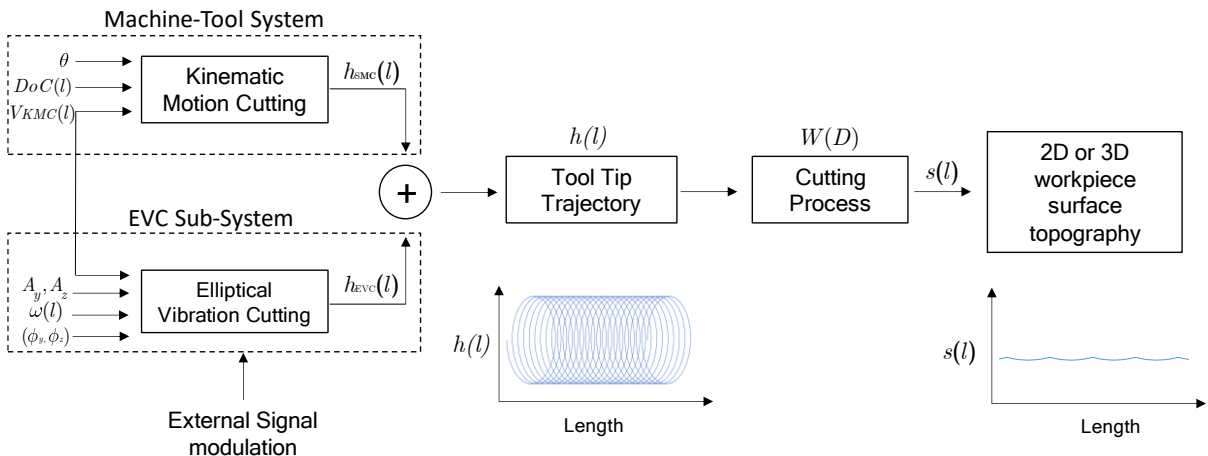


Figure 3: Analytical model of the EVASPC kinematics.

The analysis of Figure 3 suggests three main phases of the EVASPC process, all modeled in the space domain, essentially as a function of length. The conversion between time (t) and space (l) domains is required because the final surface profile remains a space, rather than time characteristic. The first phase of the framework is responsible for the summation of the slow and ultrafast components of the motion that can be represented graphically through the trochoid shown in Figure 3. Of note, the simple summation of terms ($h(l) = h_{SMC}(l) + h_{EVC}(l)$) used throughout the current study represents in fact only a first geometric and rather simplistic approximation in a sense that it disregards the effect of stability of the cutting process on resulting surface topography. However, that remains another future possible extension direction. The second phase of the framework is concerned with

the transformation of tool tip trajectory $h(l)$ into cut profile $s(l)$, a process that involves the application of the differential operator (D) on the cutting process ($W(D)$). Finally, the resulting surface topography can be calculated by performing the Boolean subtraction of the swept envelope of the tool $s(l)$ from the pre-cut workpiece volume (assumed perfectly flat in the current study). The relative positioning between the swept envelope and the workpiece surface is controlled by DoC (assumed constant).

The inherent assumption behind the aforementioned consideration is that the trochoidal swept envelope of the tool is identically replicated in the workpiece. Nonetheless, when the attack angle of the tool into the workpiece is larger than the clearance angle, undesirable interferences will be present [14]. This situation was mitigated in the current study through a judicious design of the cutting tool.

3 PROPOSED CAD/CAM FRAMEWORK

In brief, the proposed framework integrates two different tools for EVASPC topography generation. On one hand, a commercial CAD software (NX) was used to generate graphical representations of the analytically determined surface topographies. On the other hand, a Matlab-based computational platform was developed to implement the analytical model outlined in the previous section.

The visualization module relies on the analytical calculations presented in Figure 3. For this purpose, six consecutive stages were implemented in the CAD platform (Figure 4).

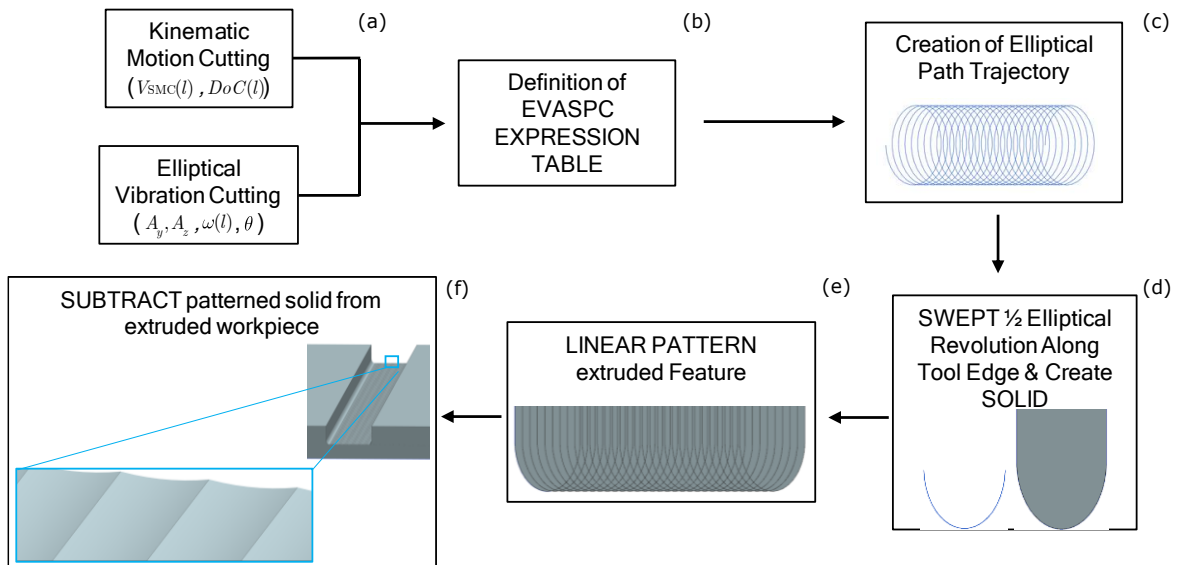


Figure 4: Visualization module: (a) analytical model, (b) determination of parametric relationships, (c) generation of elliptical tool path, (d) Boolean 'cutter', (e) replicated Boolean 'cutter', and (f) subtraction.

The core of the visualization module is represented by the required parametrizations/relationships between the geometric elements of the swept tool trajectory (Equation (2.3)). Once the discrete points of the trajectory were determined, a spline was used to interpolate them (Figure 4d). The generated curve was then converted into a solid (Figure 4d), replicated with the preset pitch of V_{SMC}/ω and over a certain span (Figure 4e) and eventually subtracted from the solid (Figure 4f). The

example illustrated in Figure 4 is based on a span of 25 μm and a pitch is 487 nm determined by $V_{\text{SMC}} = 1200 \text{ mm/min}$ and $\omega = 41 \text{ kHz}$ [2].

While explicit and extremely clear in terms of output, the CAD-based module is typically unable to appropriately handle geometric features that are different by two to three orders of magnitude. More specifically, while the geometric features of the functional surface are usually in the hundreds of microns domain, the surface finish to be generated on their facets by means of EVASPC typically falls under the 20 nm range. Because of this, it is often preferable to rely on a 'pure' numerical tool that might have limited 2D profile plotting capabilities but is capable of handling a broad range of input EVASPC parameters. To address this, a MATLAB-based module was developed (Figure 5).

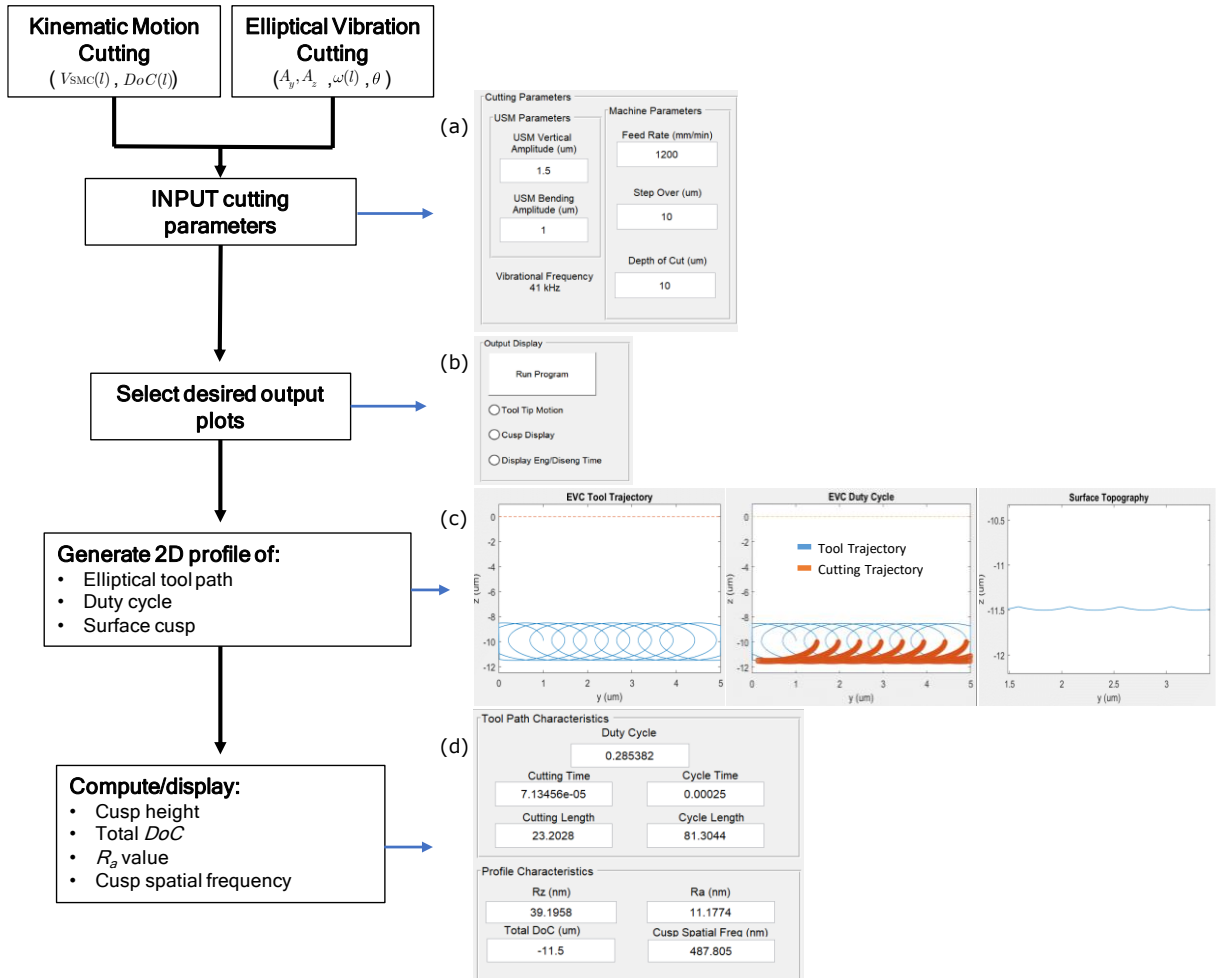


Figure 5: Computational module: (a) cutting parameters input, (b) output selection, (c) sample output plots, and (d) sample output characteristics.

This computational tool was designed to generate two primary outcomes: three 2D plots (Figure 5c) and numerical profile characteristics (Figure 5d). The tool trajectory in Figure 5c left represents nothing but the trochoid motion determined by the formulas in Equation (2.3). This plot was created in a similar fashion to the one in Figure 4c in a sense that a vector of parametrically incremented

points were used to capture the length of the specified plot (i.e., workpiece length). By contrast, duty cycle (middle plot in Figure 5c)), represents the ratio between the length of trajectory when tool is engaged with workpiece (orange region) and the total length of tool trajectory (blue region). Both tool trajectory and duty cycle are known to play an important role on cutting forces, tool-wear rate, and the surface profile [11]. The third output plot in Figure 5c (predicted surface profile) offers an important metric that can be validated by means of physical cutting trials. The 2D surface profile is calculated similar to the duty cycle in a sense that a loop structure is initiated when an intersection between y and z data points occurs. The 'workpiece engaged' portion of the loop is defined until the next intersection point. All 'cusp-to-cusp' points are stored in order to reconstruct the surface profile (i.e., the right plot shown in Figure 5c).

One important metric that can be used to check the correspondence between numerical and physical profiles is constituted by the average 2D roughness R_a to be calculated according to known formulations [3]. Of note, the calculated/analytically derived R_a value has more of a theoretical importance since it represents the lowest obtainable roughness for the chosen EVASPC process. However, any deviations from the theoretical model caused by tool geometry, wear, chatter, etc. will do nothing but increase the physical surface roughness.

4 SIMULATION RESULTS

The developed CAD/CAM framework can be used to predict various EVASPC-generated surface topographies to become the baseline for future experimental trials. While the term computer-aided manufacturing (CAM) might be somewhat of a misnomer in this particular context, it is perhaps worth emphasizing that a certain amount of overlap exists between the tasks fulfilled by a conventional CAM system and those of the proposed framework. Nonetheless, the intricacy of the geometry/surface topography generated by means of the EVASPC technique surpasses by several levels of complexity those fabricated by means of more or less traditional machining/micromachining methods. To elaborate a bit further on this idea, it will be emphasized here that whereas in the case of conventional machining/micromachining, the shape of the workpiece is almost never a concern since the goal of the fabrication process is in fact to replicate – as accurately as possible – the idealized CAD geometry, it is almost impossible to adequately imagine/predict the final topography to be produced through a certain combination of EVASPC parameters. Because of this, the aforementioned framework represents somewhat of a combined CAD/CAM system that is capable of simultaneously modeling/representing/predicting the geometry to be generated as well as to control the tool path trajectory.

		EVASPC Parameters				
		V_{SMC} (mm/min)	A_y, A_z ($\mu\text{m}, \mu\text{m}$)	(ϕ_y, ϕ_z) ($^\circ, ^\circ$)	DoC (μm)	ω (kHz)
Implementation	1	1200	(2,3)	0	10	41
	2	Variable (1200, 960, 1200)	(2,3)	0	10	41
	3	1200	Variable (2,6)	0	10	41
	4	1200	(2,3)	Variable (45,0)	10	41

Table 2: EVASPC parameters used in simulation tests.

To demonstrate the versatility of the developed framework, four different surface topographies will be simulated further, each corresponding to one of the four EVC implementations presented in Section 2. While the geometric differences between the four simulated implementations are rather evident, it will be emphasized here that they are all a direct consequence of the selected process parameters (Table 2).

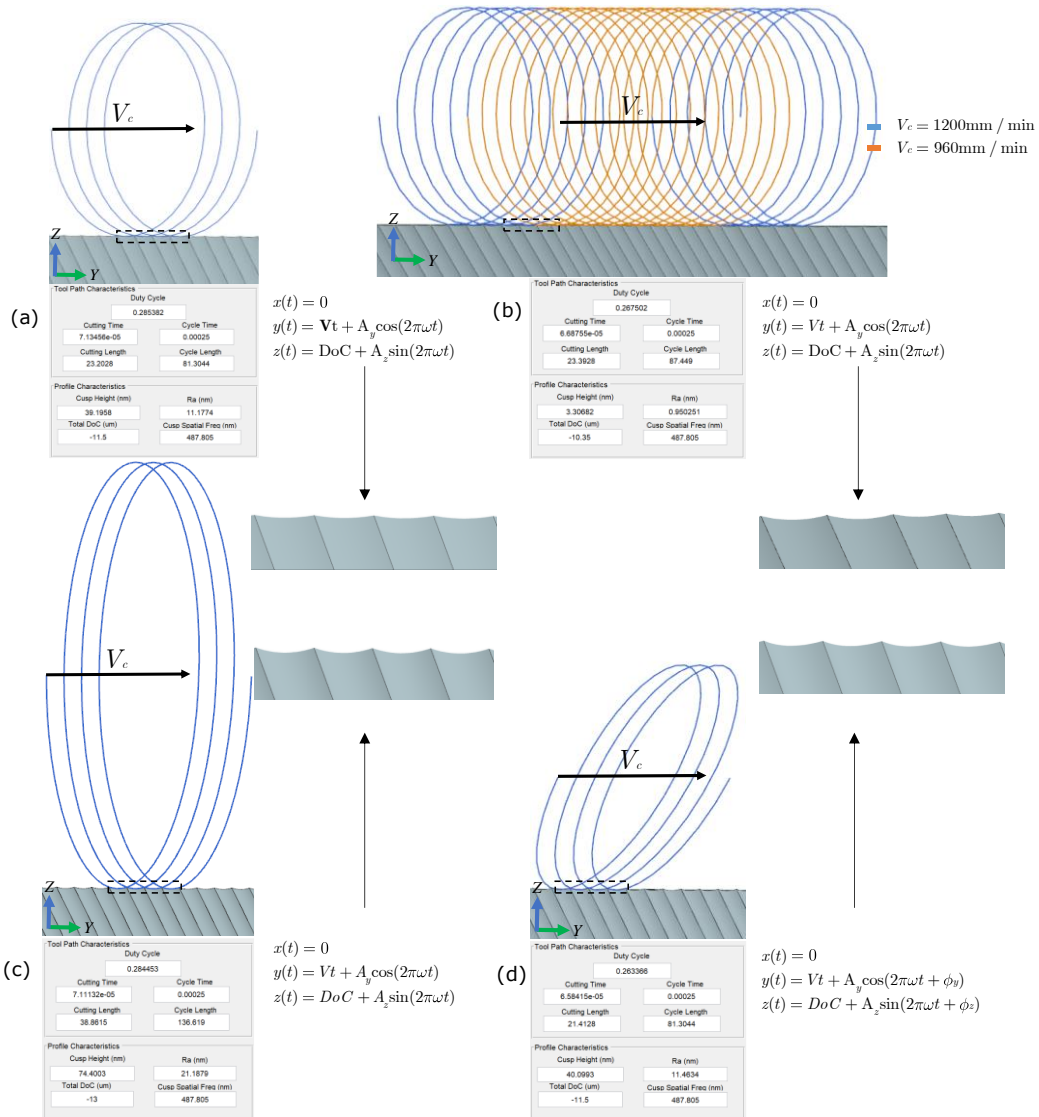


Figure 6: EVASPC simulation examples: (a) constant cutting conditions (Implementation 1), (b) modulated feed rate (Implementation 2), (c) modulated EV amplitudes (Implementation 3), and (d) modulated phase shift (Implementation 4).

More specifically, the tool path in Figure 6a demonstrates Implementation 1 (cutting parameters remain constant across the cutting length). By contrast, Figure 6b suggests the effect of a linearly variable feed rate V_{SMC} (Implementation 2), where feed decreases from 1200 mm/min to 960 mm/min and then again increases back to 1200 mm/min, while all other parameters remain constant. This supplementary 'degree of freedom' of the framework enables the possibility to areally-control the distribution of a periodical structure. Furthermore, Figure 6c implies that the ability to independently control the two vibrational amplitudes (A_y and A_z) enable changes in DoC . This is equivalent with the capability to generate a 2½D surface topography (Implementation 3). Finally, Implementation 4 – arguably the most complex one – represents a consequence of tuning/altering

the orientation of the ellipse itself (Figure 6d). The key parameter for the latter strategy is constituted by the phase shift between bending and longitudinal components of the elliptical vibrations ((ϕ_y, ϕ_z)) that can modify the elliptical locus between forward-tilted, vertically oriented (traditional EVC), and back-tilted. It is important to remember that ϕ_y and ϕ_z are relative angles with respect to each other. Because of this, a common approach involves the implementation of a non-zero value for one or the other, but not both. Figure 6d demonstrates a forward-tilted orientation of the ellipse.

5 PHYSICAL TESTS

Validation of the simulated results created by means of the proposed framework is crucial for determination of system accuracy, flexibility and general capabilities. The current section will demonstrate the use of the framework towards the fabrication of several samples associated with Implementations 1, 2 and 3. Of note, all three could be regarded as exemplifications of 'process implementations', meaning that one dominant parameter will be controlled whereas some of the others have been altered to obtain better results.

The first practical example presented herein focuses on the generation of a mirror-like, optical-quality surface on top of a ferrous sample made of P20 tool steel (Figure 7). As alluded in Section 1, steel and other hard-to-cut materials are particularly difficult to cut with diamond tools (typically due to the inherent graphitization or chipping of the cutting edge). Figure 7a depicts an EVASPC-generated sample ($55 \times 55 \text{ mm}^2$) capable to demonstrate optical surface quality characteristics. More specifically, while larger surface patches (Figure 7b) exhibited larger areal roughness values ($S_a = 37.78 \text{ nm}$), smaller ones were characterized by $S_a = 13.93 \text{ nm}$ (Figure 14b). Specific postprocessing procedures were used to level and filter the raw topographic data (ISO 4288, ASME 46.1). For reference purposes, it will be mentioned here that the industry standard for mirror-like surface finish is $R_a < 100 \text{ nm}$ while superfinishing – the hallmark surface finishing process – is capable of $R_a \approx 25 \div 200 \text{ nm}$ [4]. Therefore, the EVASPC-produced sample significantly exceeds this threshold, not only for a chosen 2D cross-section – conventionally characterized by means of average surface roughness (R_a) – but also for the entire 3D area as characterized by the average areal roughness (S_a). These results underscore once more the precision and reliability of the employed EVASPC process.

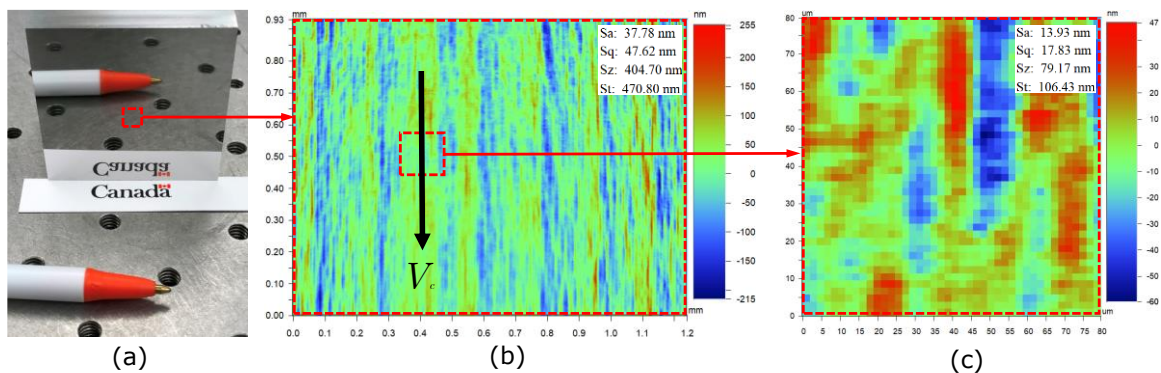


Figure 7: Application of EVASPC on ferrous materials: (a) overview of optical surface quality, (b) surface topography for a $1.2 \times 0.9 \text{ mm}^2$ patch, and (c) surface topography for a $80 \times 80 \mu\text{m}^2$ patch.

The second EVASPC-generated sample (Figure 8), demonstrates the use of Implementation 2 (controlled feed rate) towards the achievement of modulated spatial frequencies. Similar to [12],

these modulate spatial frequencies were tuned to match the wavelength of the visible light spectrum, thus producing a diffraction grating effect on the surface of the workpiece (Figure 8a). The additional tuning added to the process – performed by changing the proportional EV amplitude in order to maintain the ellipse as vertical as possible – has enabled an enhanced control of the resulting microstructure.

The third sample (Figure 9) demonstrates EVASPC fabrication of saw-tooth structures with height and width of $2.5\ \mu\text{m}$ and $14\ \mu\text{m}$, respectively. As mentioned in Implementation 3, these surface structures are achieved by modulating the EV amplitudes (A_y, A_z) across the cutting length, essentially by stepping down with increasing ellipse sizes as tool descends further along the saw-tooth slope. Similar to [13], this technique can produce surfaces used in hydrodynamic and aerodynamic applications.

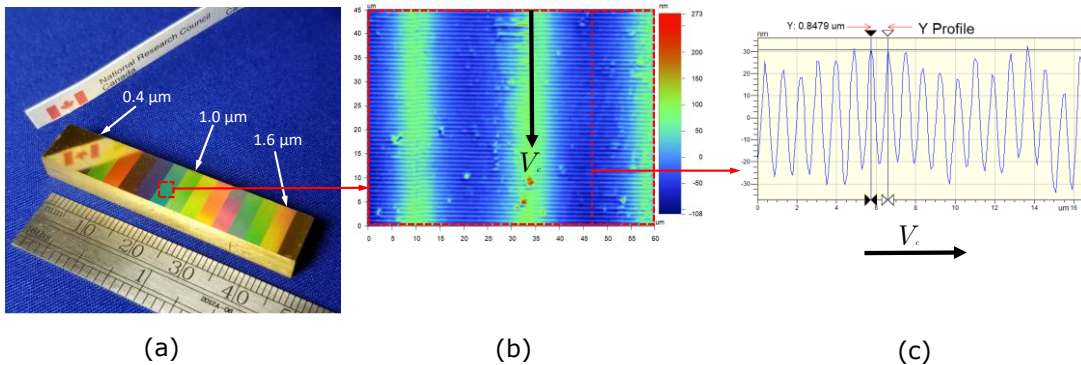


Figure 8: EVASPC of brass with $0.4 \dots 1.6\ \mu\text{m}$ diffraction gratings: a) sample overview, b) surface topography for $0.9\ \mu\text{m}$ grating, and c) corresponding surface profile.

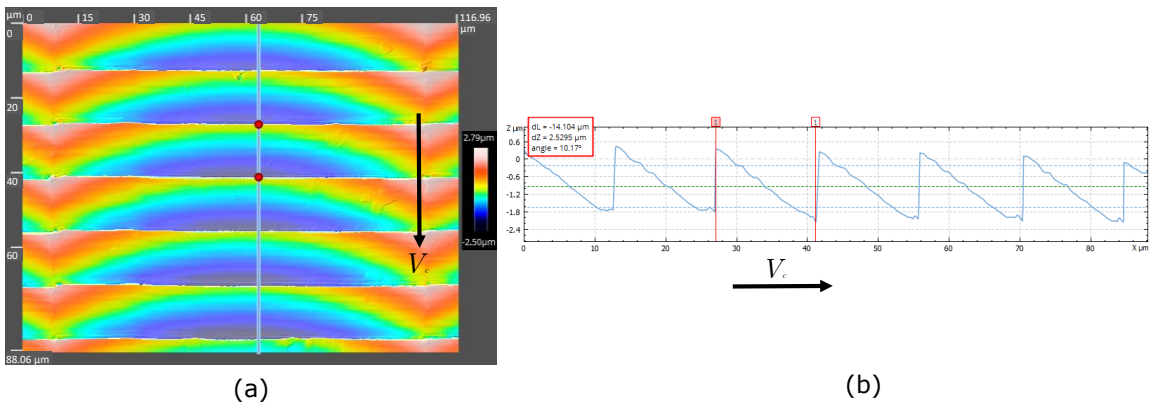


Figure 9: EVASPC-generated saw-tooth structures ($14\ \mu\text{m} \times 2.5\ \mu\text{m}$): a) surface topography, and b) profile characteristics.

The samples shown in this section demonstrate the utility of the developed framework towards the fabrication of the intended physical samples.

6 SUMMARY AND CONCLUSIONS

The CAD/CAM framework proposed in this study represents one of the first attempts to integrate and capture various EVC strategies that were previously reported. The two principal modules developed for this purpose (CAD and computational) were built on the analytical formulation of EVASPC that essentially merges its two primary motions namely the 'slow' motion of the CNC stage and the 'ultrafast' motion of the EV system. The models produced by means of the developed framework demonstrated its suitability to microstructure design as well as further to its fabrication. Following up on that, the physical tests performed have demonstrated that the EVASPC is equally applicable to the generation high quality flat surfaces on ferrous materials as well as to the fabrication of precise microstructures with diverse surface functionalization roles.

Future extensions of this work will attempt to perform more in-depth comparisons between the modeling and experimental results. Furthermore, while it becomes increasingly clear that EVASPC applications are almost limitless in terms of the geometry complexity that can be fabricated, the practical significance of many EVASPC-generated microstructures remains to be uncovered in the future.

ACKNOWLEDGEMENTS

The work presented in this study was the result of the collaboration between Western University (London, Ontario) and National Research Council of Canada (London, Ontario). Partial financial support was also provided by Natural Sciences and Engineering Research Council (NSERC) of Canada. The authors would also like to thank Mr. Nicolas Milliken and Dr. Mohammed Tauhiduzzaman of National Research Council of Canada (London, Ontario) for their participation in the microfabrication of samples presented in this study.

Nikolai Farrus, <https://orcid.org/0000-0002-7021-1458>
 O. Remus Tutunea-Fatan, <https://orcid.org/0000-0002-1016-5103>
 Evgueni Bordatchev, <https://orcid.org/0000-0003-2347-6338>

REFERENCES

- [1] Abdulbari, H. A.; Mahammed, H. D.; Hassan, Z. B.: Bio-Inspired Passive Drag Reduction Techniques: A Review, *ChemBioEng Reviews*, 2, 2015, 185-203. <http://dx.doi.org/http://dx.doi.org/10.1002/cben.201400033>
- [2] Bai, W.; Sun, R.; Gao, Y.; Leopold, J.: Analysis and modeling of force in orthogonal elliptical vibration cutting, *The International Journal of Advanced Manufacturing Technology*, 83, 2016, 1025-1036. <http://dx.doi.org/http://dx.doi.org/10.1007/s00170-015-7645-6>
- [3] Bhushan, B.: Surface roughness analysis and measurement techniques, in "Modern Tribology Handbook, Two Volume Set", 2000, CRC press, 79-150. 10.1201/9780849377877-10
- [4] Davim, J. P.: Surface integrity in machining, Springer, 2010.
- [5] Guo, P.; Ehmann, K. F.: An analysis of the surface generation mechanics of the elliptical vibration texturing process, *International Journal of Machine Tools and Manufacture*, 64, 2013, 85-95. <http://dx.doi.org/https://doi.org/10.1016/j.ijmachtools.2012.08.003>
- [6] Guo, P.; Lu, Y.; Ehmann, K. F.; Cao, J.: Generation of hierarchical micro-structures for anisotropic wetting by elliptical vibration cutting, *CIRP Annals*, 63, 2014, 553-556. <http://dx.doi.org/10.1016/j.cirp.2014.03.048>
- [7] Hamilton, B. W.; Hussein, S.; Milliken, N.; Tutunea-Fatan, O. R.; Bordatchev, E. V.: Fabrication of right triangular prism retroreflectors through 3½-axis ultraprecise single point inverted cutting, *Computer-Aided Design and Applications*, 14, 2017, 693-703. <http://dx.doi.org/http://dx.doi.org/10.1080/16864360.2016.1273586>
- [8] Luo, Y.; Liu, Y.; Anderson, J.; Li, X.; Li, Y.: Improvement of water-repellent and hydrodynamic drag reduction properties on bio-inspired surface and exploring sharkskin effect mechanism,

- Applied Physics A, 120, 2015, 369-377. <http://dx.doi.org/> <http://dx.doi.org/10.1007/s00339-015-9198-9>
- [9] Milliken, N.; Hamilton, B.; Hussein, S.; Tutunea-Fatan, O. R.; Bordatchev, E.: Enhanced bidirectional ultraprecise single point inverted cutting of right triangular prismatic retroreflectors, Precision Engineering, 52, 2018, 158-169. <http://dx.doi.org/> <http://dx.doi.org/10.1016/j.precisioneng.2017.12.002>
- [10] Shamoto, E.; Moriwaki, T.: Ultraprecision diamond cutting of hardened steel by applying elliptical vibration cutting, CIRP Annals-Manufacturing Technology, 48, 1999, 441-444. <http://dx.doi.org/> [http://dx.doi.org/10.1016/S0007-8506\(07\)63222-3](http://dx.doi.org/10.1016/S0007-8506(07)63222-3)
- [11] Sui, H.; Zhang, X.; Zhang, D.; Jiang, X.; Wu, R.: Feasibility study of high-speed ultrasonic vibration cutting titanium alloy, Journal of Materials Processing Technology, 247, 2017, 111-120. <http://dx.doi.org/> <http://dx.doi.org/10.1016/j.jmatprotec.2017.03.017>
- [12] Yang, Y.; Pan, Y.; Guo, P.: Structural coloration of metallic surfaces with micro/nano-structures induced by elliptical vibration texturing, Applied Surface Science, 402, 2017, 400-409. <http://dx.doi.org/> <http://dx.doi.org/10.1016/j.apsusc.2017.01.026>
- [13] Zhang, J.; Cui, T.; Ge, C.; Sui, Y.; Yang, H.: Review of micro/nano machining by utilizing elliptical vibration cutting, International Journal of Machine Tools and Manufacture, 106, 2016, 109-126. <http://dx.doi.org/> <https://doi.org/10.1016/j.ijmachtools.2016.04.008>
- [14] Zhang, J.; Suzuki, N.; Shamoto, E.: Investigation on machining performance of amplitude control sculpturing method in elliptical vibration cutting, Procedia Cirp, 8, 2013, 328-333. <http://dx.doi.org/> <http://dx.doi.org/10.1016/j.procir.2013.06.111>
- [15] Zhang, J.; Suzuki, N.; Wang, Y.; Shamoto, E.: Ultra-precision nano-structure fabrication by amplitude control sculpturing method in elliptical vibration cutting, Precision Engineering, 39, 2015, 86-99. <http://dx.doi.org/> <https://doi.org/10.1016/j.precisioneng.2014.07.009>
- [16] Zhang, X.; Kumar, A. S.; Rahman, M.; Liu, K.: Modeling of the effect of tool edge radius on surface generation in elliptical vibration cutting, The International Journal of Advanced Manufacturing Technology, 65, 2013, 35-42. <http://dx.doi.org/> <https://doi.org/10.1007%2Fs00170-012-4146-8>